Preparation and Reaction Chemistry of Trimethylsilyl Derivatives of Tantalum. X-ray Structures of d^0 (η^5-C_5Me_5)Ta($SiMe_3$)Cl_3 and d^1 (η^5-C_5Me_5)Ta($SiMe_3$)(PMe_3)Cl_2

John Arnold, David N. Shina, and T. Don Tilley*

Chemistry Department, D-006, University of California at San Diego, La Jolla, California 92093

Atta M. Arif

Department of Chemistry, The University of Texas at Austin, Austin, Texas 78712

Received February 28, 1986

The preparation of Cp*Ta($SiMe_3$)Cl_3 (1, Cp* = η^5-C_5Me_5) from Cp*$TaCl_4$ and Al($SiMe_3$)$_3$·OEt_2 is reported. Compound 1 is converted to the derivatives Cp*Ta($SiMe_3$)(OR)Cl_2 (2, R = $SiMe_3$; 3, R = CMe_3) upon treatment with $KOSiMe_3$ or $LiOCMe_3$, respectively. Reaction of 1 with MeMgBr (3 equiv) produces Cp*Ta($SiMe_3$)Me_3 (4). Donor ligands induce reductive elimination of Me_3SiCl from 1. In the case of alkyne addition, the resulting tantalum(III) products are Cp*Ta(RC≡CR′)Cl_2 (R = R′ = Me_3Si, Ph, Me; R = Ph, R′ = H). When the incoming ligand is PMe_3, it appears that an initially formed tantalum(III) product reacts with starting material to afford the tantalum(IV) silyl Cp*Ta($SiMe_3$)(PMe_3)Cl_2 (8) and Cp*$TaCl_4$(PMe_3) via a series of redox transformations. Complexes 1 and 8 have been structurally characterized. Dark green crystals of 1 belong to space group $P2_1/c$ with unit cell dimensions a = 15.133 (2) Å, b = 8.522 (2) Å, c = 14.157 (1) Å, β = 91.923 (1)°, V = 1824.7 (5) Å^3, and Z = 4. The final R value refined against 1959 data was 3.84%. The paramagnetic d^1 silyl 8 also crystallizes in the monoclinic space group $P2_1/c$ with a = 13.3309 (14) Å, b = 10.3770 (10) Å, c = 16.1017 (25) Å, β = 94.061 (10)°, V = 2221.8 (8) Å^3, and Z = 4. The final R value for 2494 data was 1.54%. Both structures exhibit a four-legged piano-stool geometry with noncrystallographic C_s symmetry. The Ta(IV)–Si bond in 8, 2.642 (1) Å, is slightly shorter than the Ta(V)–Si bond in 1, 2.669 (4) Å. These distances are discussed with respect to electron density at the transition-metal center and Ta–Si π-bonding.

Introduction

Since the first transition-metal silyl derivative CpFe(CO)$_2$$SiMe_3$ (Cp = η^5-C_5H_5) was reported by Wilkinson in 1956,[1] numerous other examples have been prepared and studied.[2] Recent advances by Gladysz and co-workers have led to some valuable synthetic routes based on iron and manganese trimethylsilyl complexes.[3] Most of the research in this area has dealt with late or low-valent transition-metal compounds, for which crystallographic studies have revealed rather short metal–silicon bonds.[2a–d,4a] These metal–silicon distances have been attributed to π-bonding between the metal and silicon.

Studies of early transition-metal silyls are less common.[4–7] Our work in this area[5,6] has led us to examine the silyl chemistry of tantalum.[6] The only previously reported tantalum silyl, Cp_2Ta($SiMe_2Ph$)H_2, was recently described by Curtis et al.[7] Herein we report the preparation of Cp*Ta($SiMe_3$)Cl_3 (1, Cp* = η^5-C_5Me_5) and some of its chemistry, including reactions that invclve reductive elimination of Me_3SiCl. Crystallographic studies on the closely related d^0 and d^1 silyls 1 and Cp*Ta($SiMe_3$)(PMe_3)Cl_2 (8) reveal the effect of electron density at the metal on the Ta–Si bond length.

Results and Discussion

Preparation and Properties of (η^5-C_5Me_5)Ta($SiMe_3$)Cl_3 (1). An attempt to prepare a tantalum silyl complex by reaction of $TaCl_5$ with the silylating agent Al($SiMe_3$)$_3$·OEt_2[8] in toluene resulted in formation of black, insoluble material. No tantalum-containing products could be isolated; the apparent decomposition products Me_3SiCl (0.86 equiv) and $Me_3SiSiMe_3$ (0.16 equiv) were detected in solution by GC. Modification of the tantalum starting material to Cp*$TaCl_4$,[9] however, allowed isolation of the air-sensitive, dark green silyl compound 1 in 58% yield (eq 1). In benzene-d_6 the $SiMe_3$ protons of 1 appear at 0.89

$$\mathrm{Cp^*TaCl_4} + \mathrm{Al(SiMe_3)_3{\cdot}OEt_2} \xrightarrow{\text{pentane}} \underset{\mathbf{1}}{\mathrm{Cp^*Ta(SiMe_3)Cl_3}} \tag{1}$$

ppm in the ^{1}H NMR spectrum (Table I), an unusually low-field shift for a metal–$SiMe_3$ derivative. In the group 4 metal–$SiMe_3$ complexes that we have prepared, the corresponding shifts are typically between 0.30 and 0.50 ppm.[5a]

Under nitrogen at room temperature, crystalline 1 is thermally and photolytically stable. Prolonged exposure of solutions of 1 to ambient fluorescent light, however, causes decomposition with elimination of Me_3SiCl (by GC). Thermolysis of 1 in benzene-d_6 solution at 90 °C leads to formation of dark green insoluble material and Me_3SiCl (70% by GC and ^{1}H NMR); decomposition is cleanly first order in 1 ($t_{1/2}$ = 26 h at 90 °C). Compound 1 is readily

---

[1] Piper, T. S.; Lemal, D.; Wilkinson, G. *Naturwissenschaften* **1956**, *43*, 129.

[2] (a) Cundy, C. S.; Kingston, B. M.; Lappert, M. F. *Adv. Organomet. Chem.* **1973**, *11*, 253. (b) Aylett, B. J. *Adv. Inorg. Chem. Radiochem.* **1982**, *25*, 1. (c) Ang, H. G.; Lau, P. T. *Organomet. Chem. Rev., Sect. A* **1972**, *8*, 235. (d) Höfler, F. *Top. Curr. Chem.* **1974**, *50*, 129. (e) Speier, J. L. *Adv. Organomet. Chem.* **1978**, *17*, 407. (f) Aylett, B. J. *J. Organomet. Chem. Libr.* **1980**, *9*, 327. (g) Curtis, M. D.; Epstein, P. S. *Adv. Organomet. Chem.* **1981**, *19*, 213. (h) Colomer, E.; Corriu, R. J. P. *Top. Curr. Chem.* **1981**, *96*, 79.

[3] Gladysz, J. A. *Acc. Chem. Res.* **1984**, *17*, 326.

[4] (a) Muir, K. W. *J. Chem. Soc. A* **1971**, 2663. (b) Kingston, B. M.; Lappert, M. F. *J. Chem. Soc., Dalton Trans.* **1972**, 69. (c) Hencken, G.; Weiss, E. *Chem. Ber.* **1973**, *106*, 1747. (d) Holtman, M. S.; Schram, E. P. *J. Organomet. Chem.* **1980**, *187*, 147. (e) Rösch, L.; Altnau, G.; Erb, W.; Pickardt, J.; Bruncks, N. *J. Organomet. Chem.* **1980**, *197*, 51.

[5] (a) Tilley, T. D. *Organometallics* **1985**, *4*, 1452. (b) Tilley, T. D. *J. Am. Chem. Soc.* **1985**, *107*, 4084.

[6] (a) Arnold, J.; Tilley, T. D. *J. Am. Chem. Soc.* **1985**, *107*, 6409. (b) Arnold, J.; Tilley, T. D.; Rheingold, A. L. *J. Am. Chem. Soc.*, in press.

[7] Curtis, M. D.; Bell, L. G.; Butler, W. M. *Organometallics* **1985**, *4*, 701.

[8] Rösch, L.; Altnau, G. *J. Organomet. Chem.* **1980**, *195*, 47.

[9] (a) Herrmann, W. A.; Kalcher, W. W.; Biersack, H.; Bernal, I.; Creswick, M. *Chem. Ber.* **1981**, *114*, 3558. (b) Sanner, R. D.; Carter, S. T.; Bruton, W. J., Jr. *J. Organomet. Chem.* **1982**, *240*, 157.

0276-7333/86/2305-2037$01.50/0

Table I. ^{1}H and ^{13}C NMR Data for New Compounds

compd	^{1}H NMR data[a]		^{13}C{^{1}H} NMR data[b]	
Cp*Ta(SiMe$_3$)Cl$_3$ (**1**)	$\mathrm{Si(C}H_3)_3$	0.89 (s)	$\mathrm{Si(}C\mathrm{H_3)_3}$	11.6
	$\mathrm{C_5(C}H_3)_5$	1.89 (s)	$\mathrm{C_5(}C\mathrm{H_3)_5}$	13.3
			$C_5\mathrm{(CH_3)_5}$	125.6
Cp*Ta(SiMe$_3$)(OSiMe$_3$)Cl$_2$ (**2**)	$\mathrm{OSi(C}H_3)_3$	0.27 (s)	$\mathrm{OSi(}C\mathrm{H_3)_3}$	2.03
	$\mathrm{Si(C}H_3)_3$	0.64 (s)	$\mathrm{Si(}C\mathrm{H_3)_3}$	9.04
	$\mathrm{C_5(C}H_3)_5$	1.89 (s)	$\mathrm{C_5(}C\mathrm{H_3)_5}$	12.7
			$C_5\mathrm{(CH_3)_5}$	122.6
Cp*Ta(SiMe$_3$)(OCMe$_3$)Cl$_2$ (**3**)	$\mathrm{Si(C}H_3)_3$	0.76 (s)		
	$\mathrm{OC(C}H_3)_3$	1.35 (s)		
	$\mathrm{C_5(C}H_3)_5$	1.92 (s)		
Cp*Ta(SiMe$_3$)Me$_3$ (**4**)[c]	$\mathrm{Si(C}H_3)_3$	0.57 (s)	$\mathrm{Si(}C\mathrm{H_3)_3}$	9.12
	$\mathrm{Ta(C}H_3)_3$	0.77 (s)	$\mathrm{C_5(}C\mathrm{H_3)_5}$	11.55
	$\mathrm{C_5(C}H_3)_5$	1.70 (s)	$C_5\mathrm{(CH_3)_5}$	117.0
Cp*CpTa(SiMe$_3$)(PMe$_3$) (**6**)[d]	$\mathrm{Si(C}H_3)_3$	0.51 (s)	$\mathrm{Si(}C\mathrm{H_3)_3}$	12.1
	$\mathrm{P(C}H_3)_3$	1.11 (d, J = 7 Hz)	$\mathrm{C_5(}C\mathrm{H_3)_5}$	13.2
	$\mathrm{C_5(C}H_3)_5$	1.77 (s)	$\mathrm{P(}C\mathrm{H_3)_3}$	25.7 (d, J = 22 Hz)
	$\mathrm{C_5}H_5$	3.96 (d, J = 2 Hz)	$C_5\mathrm{H_5}$	84.9
			$C_5\mathrm{(CH_3)_5}$	97.0
Cp*Cl$_2$Ta(Me$_3$SiC≡CSiMe$_3$) (**7**)[d]	$\mathrm{Si(C}H_3)_3$	0.33 (s)	$\mathrm{Si(}C\mathrm{H_3)_3}$	1.70
	$\mathrm{C_5(C}H_3)_5$	1.77 (s)	$\mathrm{C_5(}C\mathrm{H_3)_5}$	12.2
			$C_5\mathrm{(CH_3)_5}$	120.2
			$\mathrm{Si}C_2\mathrm{Si}$	247.9

[a] Chemical shifts are in ppm, referenced to C$_6$D$_5$H (δ 7.15) at 360 MHz and 22 °C in C$_6$D$_6$ except where noted. [b] In C$_6$D$_6$ at 50.3 MHz and 22 °C, referenced to C$_6$D$_6$ at 128.0 ppm except where noted. [c] Methyl ligand carbons not detected in ^{13}C{^{1}H} spectrum at 22 °C. [d] ^{1}H NMR recorded at 300 MHz; ^{13}C NMR recorded at 75 MHz.

hydrolyzed to HSiMe$_3$ (quantitative by ^{1}H NMR) and a yellow powder. Although complete characterization of the latter product was hindered by its low solubility in common solvents, we noted that the same product is formed upon hydrolysis of Cp*TaCl$_4$. On the basis of IR data, this compound appears to be either [Cp*TaCl$_2$(OH)]$_2$O or [Cp*TaCl$_3$(OH$_2$)]$_2$O. Hydrolysis of (η^5-C$_5$H$_4$Me)NbCl$_4$ has been shown to give [(η^5-C$_5$H$_4$Me)NbCl$_3$(OH$_2$)]$_2$O.[10]

Chloride Substitution Reactions of 1. Attempts to further substitute the chloride ligands in **1** with silyl groups were unsuccessful; no reaction took place between **1** and excess Al(SiMe$_3$)$_3$·OEt$_2$ upon stirring for 3 days at room temperature in benzene. Refluxing this solution produced brown tar-like materials that could not be characterized. Reaction of **1** with LiSi(SiMe$_3$)$_3$·3THF[11] in pentane led to complex oily mixtures from which no pure products could be isolated.

Treatment of **1** with 1 equiv of KOSiMe$_3$ or LiOCMe$_3$ produces the siloxide and alkoxide derivatives **2** and **3**, respectively (eq 2). The deep red compounds **2** and **3** are

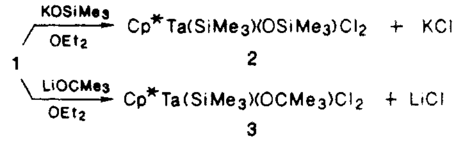

$$\mathbf{1}\ \begin{cases}\xrightarrow[\mathrm{OEt_2}]{\mathrm{KOSiMe_3}} \underset{\mathbf{2}}{\mathrm{Cp^*Ta(SiMe_3)(OSiMe_3)Cl_2}} + \mathrm{KCl} \\ \xrightarrow[\mathrm{OEt_2}]{\mathrm{LiOCMe_3}} \underset{\mathbf{3}}{\mathrm{Cp^*Ta(SiMe_3)(OCMe_3)Cl_2}} + \mathrm{LiCl}\end{cases} \qquad (2)$$

highly pentane-soluble and air-sensitive. Whereas **2** is thermally stable as a solid or in solution at room temperature, **3** is not and must be stored at low temperature (−45 °C). Reaction of **1** with more than 1 equiv of KOSiMe$_3$ or LiOCMe$_3$ resulted in complex reaction mixtures which yielded no pure products upon workup.

Reaction of **1** with 3 equiv of MeMgBr in OEt$_2$ at −78 °C affords the mixed alkyl/silyl Cp*Ta(SiMe$_3$)Me$_3$ (**4**) in high yield (eq 3). This compound is unstable over long

$$\mathbf{1} + 3\mathrm{MeMgBr} \xrightarrow[-78\ ^\circ\mathrm{C}]{\mathrm{OEt_2}} \underset{\mathbf{4}}{\mathrm{Cp^*Ta(SiMe_3)Me_3}} \qquad (3)$$

periods at 25 °C but can be safely stored at −20 °C. Heating benzene-d_6 solutions of **4** at 90 °C for 3 h produces HSiMe$_3$ (quantitatively by ^{1}H NMR) and unidentified tantalum-containing products. In common with other Ta(V) "four-legged piano-stool" complexes, **4** is fluxional in solution, exhibiting a singlet for the three methyl ligands at room temperature (δ 0.77 (9 H)) and a pair of singlets (δ 1.25 (6 H), 0.60 (3 H)) at −80 °C (^{1}H NMR, toluene-d_8). The $\Delta G^\ddagger$ for this process is 12.5 ± 0.5 kcal mol^{-1}, similar to that reported for the related compound Cp*TaMe$_3$Cl-($\Delta G^\ddagger$ = 13.6 ± 1.4 kcal mol^{-1}).[12]

Compound **1** reacts with 1 or 2 equiv of NaCp in diethyl ether to give the reduced tantalum(IV) species Cp*CpTa(SiMe$_3$)Cl (**5**) as the only isolable product (eq 4). This pentane-soluble, paramagnetic complex is further reduced by Na/Hg in the presence of trimethylphosphine to the tantalum(III) silyl Cp*CpTa(SiMe$_3$)(PMe$_3$) (**6**, eq 5).

$$\mathbf{1} + 2\mathrm{NaCp} \xrightarrow{\mathrm{OEt_2}} \underset{\mathbf{5}}{\mathrm{Cp^*CpTa(SiMe_3)Cl}} \qquad (4)$$

$$\mathbf{5} + \mathrm{Na(Hg)} + \mathrm{PMe_3} \xrightarrow{\mathrm{THF}} \underset{\mathbf{6}}{\mathrm{Cp^*CpTa(SiMe_3)(PMe_3)}} \qquad (5)$$

Reactions of 1 with Donor Ligands. Given the electron-deficient nature of **1** (formally a 14-electron complex), we assumed it would readily add donor ligands to form complexes analogous to the known Cp*TaCl$_4$-(PMe$_3$).[12] Such adduct formation has not yet been observed.

Refluxing a benzene solution of **1** and diphenylacetylene (1 equiv) for 2 days results in formation of the known compound Cp*Cl$_2$Ta(PhC≡CPh)[13] in high yield. Analysis of the volatiles from the reaction (by GC and ^{1}H NMR) revealed Me$_3$SiCl as an additional product. Under similar conditions, bis(trimethylsilyl)acetylene reacts with **1** in ca. 4 h to produce Cp*Cl$_2$Ta(Me$_3$SiC≡CSiMe$_3$) (**7**) and Me$_3$SiCl. Reactions of **1** with phenylacetylene and 2-butyne also give Me$_3$SiCl and the corresponding alkyne

---

(10) Bunker, M. J.; DeCain, A.; Green, M. L. H.; Moreau, J. J. E.; Siganporia, N. *J. Chem. Soc., Dalton Trans.* **1980**, 2155.

(11) Gutekunst, G.; Brook, A. G. *J. Organomet. Chem.* **1982**, *225*, 1.

(12) McLain, S. J.; Wood, C. D.; Schrock, R. R. *J. Am. Chem. Soc.* **1979**, *101*, 4558.

(13) Smith, G.; Schrock, R. R.; Churchill, M. R.; Youngs, W. J. *Inorg. Chem.* **1981**, *20*, 387.

Scheme I

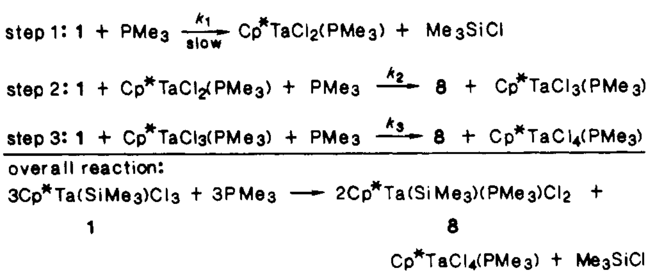

complexes $Cp^*Cl_2Ta(PhC{\equiv}CH)$[13] and $Cp^*Cl_2Ta(MeC{\equiv}CMe)$,[13] as determined by ^1H NMR. The rates of these reactions (eq 6) depend upon both the nature and concentration of alkyne and follow the order $MeC{\equiv}CMe > Me_3SiC{\equiv}CSiMe_3 > PhC{\equiv}CH >> PhC{\equiv}CPh$. Although fluctuations in the rate data prevented an accurate kinetic treatment (for all four alkyne reactions), the qualitative ordering of rates was readily apparent. These results suggest an associative mechanism in which coordination of alkyne to 1 induces reductive elimination of Me_3SiCl. We observed similar reductive eliminations of Me_3SiCl in the reactions of CO with 1[6a] and $Cp_2Ti(SiMe_3)Cl$.[14] Ligand-induced reductive eliminations are also known to occur in d^0 zirconium alkyl–hydride complexes.[15]

$$1 + RC{\equiv}CR' \xrightarrow[\Delta]{\text{benzene}} Cp^*Cl_2Ta(RC{\equiv}CR') + Me_3SiCl \qquad (6)$$

$$R = R' = Ph, SiMe_3, Me; R = Ph, R' = H$$

The ^1H NMR spectrum of 1 in benzene-d_6 is unaffected by addition of triethylphosphine, tricyclohexylphosphine, or triphenylphosphine, and attempts at preparative scale reactions led only to isolation of starting materials after several days at room temperature. Addition of trimethylphosphine (1 equiv) to a benzene solution of 1, however, results in a gradual color change from green to dark red over the course of 1 day. The reaction proceeds faster with excess trimethylphosphine. Workup and analysis of the reaction mixture led to isolation of $Cp^*Ta(SiMe_3)(PMe_3)Cl_2$ (8, 55% isolated yield), $Cp^*TaCl_4(PMe_3)$[12] (14% isolated yield), and Me_3SiCl (30% yield by GC). These yields suggest the stoichiometry shown in eq 7. Pentane-soluble, dark red, paramagnetic (d^1) 8 has been characterized by X-ray crystallography (vide infra). The ESR spectrum of 8 shows an 8-line pattern (0.01 M, benzene-d_6, 25 °C, $g_{av} = 1.961$, $a_{av} = 9.99 \times 10^{-3}$ cm^{-1}) due to tantalum coupling (^{181}Ta, 99.988%, $I = {}^7/_2$).

$$\underset{1}{3Cp^*Ta(SiMe_3)Cl_3} + 3PMe_3 \xrightarrow{C_6H_6} \underset{8}{2Cp^*Ta(SiMe_3)(PMe_3)Cl_2} + Cp^*TaCl_4(PMe_3) + Me_3SiCl \qquad (7)$$

Formation of the products in eq 7 are explained by the sequence of reactions in Scheme I. The rate-determining step appears to be phosphine-induced reductive elimination of Me_3SiCl to form $Cp^*TaCl_2(PMe_3)$. This tantalum(III) intermediate then reacts with 1 and trimethylphosphine to produce two tantalum(IV) species, 8 and a second intermediate, $Cp^*TaCl_3(PMe_3)$.[12] In the final step chlorine transfer from 1 to $Cp^*TaCl_3(PMe_3)$ affords another equivalent of 8 and the tantalum(V) product $Cp^*TaCl_4(PMe_3)$.

Scheme II

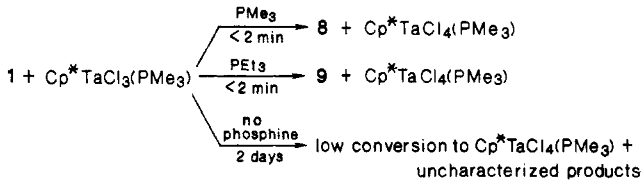

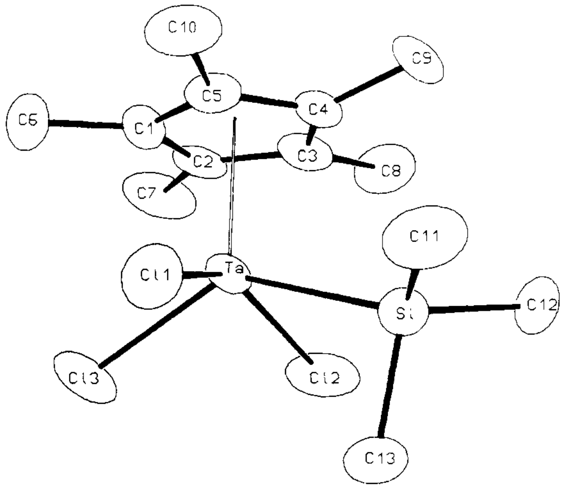

Figure 1. ORTEP view of $Cp^*Ta(SiMe_3)Cl_3$ (1) showing atom-labeling scheme.

The last reaction in Scheme I can be tested since the reactants are isolable compounds. Reaction of 1 with $Cp^*TaCl_3(PMe_3)$ and trimethylphosphine rapidly proceeds (<2 min at room temperature) to a 1:1 mixture of the predicted products (Scheme II). This reaction requires added phosphine. In the absence of trimethylphoshine (or, if triphenylphosphine is employed instead), reaction proceeds very slowly; large amounts of starting materials remain after several days at room temperature, along with small amounts of $Cp^*TaCl_4(PMe_3)$ and uncharacterized insoluble materials. With triethylphosphine, which does not react with 1 in the absence of $Cp^*TaCl_3(PMe_3)$, only $Cp^*Ta(SiMe_3)(PEt_3)Cl_2$ (9) and $Cp^*TaCl_4(PMe_3)$ were formed; neither 8 nor $Cp^*TaCl_4(PEt_3)$ could be detected among the reaction products. (The tantalum(IV) silyl 9 was prepared independently by reduction of 1 in the presence of triethylphosphine—see Experimental Section.) Although the detailed mechanism of this reaction is not known, these results suggest that incoming phosphine is required for chlorine transfer from 1 to $Cp^*TaCl_3(PMe_3)$. In addition, the reactions in Scheme II imply that the silyl group stabilizes the tantalum(IV) metal center to a greater extent than chlorine. This effect may be due in part to the π-acceptor character of the silicon (vide infra). Alternatively, the chloride ligand, acting as a better π-donor, stabilizes the tantalum(V) center to a higher degree.

Description of the Structures of 1 and 8. Both structures consist of independent molecules that adopt the "four-legged piano-stool" geometry invariably observed for complexes of the type $CpML_4$.[16] ORTEP views are provided in Figures 1 and 2, and relevant geometrical parameters are given in Tables III–VI. For compound 8, the first d^1 silyl complex to be structurally characterized, the identity

---

(14) Tilley, T. D.; Campion, B. K.; Falk, J., manuscript in preparation.

(15) (a) McAlister, D. R.; Erwin, D. K.; Bercaw, J. E. *J. Am. Chem. Soc.* **1978**, *100*, 5966. (b) Yoshifjui, M.; Gell, K. I.; Schwartz, J. *J. Organomet. Chem.* **1978**, *153*, C15. (c) Gell, K. I.; Schwartz, J. *J. Chem. Soc., Chem. Commun.* **1979**, 244. (d) Gell, K. I.; Schwartz, J. *J. Am. Chem. Soc.* **1981**, *103*, 2687.

(16) (a) Kubáček, P.; Hoffmann, R.; Havlas, Z. *Organometallics* **1982**, *1*, 180. (b) Barnett, K. W.; Slocum, D. W. *J. Organomet. Chem.* **1972**, *44*, 1.

Table II. Cell Constants and Data Collection Parameters for the X-ray Diffraction Experiments

	1 (25 °C)	8 (25 °C)
	(A) Crystal Parameters	
a, Å	15.133 (2)[a]	13.3309 (14)[b]
b, Å	8.522 (2)	10.3770 (10)
c, Å	14.157 (1)	16.1017 (25)
β, deg	91.923 (1)	94.061 (10)
V, Å^3	1824.7 (5)	2221.8 (8)
space group	$P2_1/c$	$P2_1/c$
Z	4	4
d_{calcd}, g cm^{-3}	1.80	1.61
μ_{calcd}, cm^{-1}	64.5	52.5
cryst size, mm	0.25 × 0.20 × 0.18	0.24 × 0.24 × 0.45
	(B) Data Measurement Parameters	
radiatn	Mo Kα (λ = 0.71073 Å)	
monochromator	highly oriented graphite	(2θ = 12.2°)
reflcns measd	$+h,+k,\pm l$	$+h,+k,\pm l$
2θ range, deg	3–48	3–45
scan type	θ–2θ	θ–2θ
scan width	$\Delta\theta$ = 0.8 + 0.350 tan θ	$\Delta\theta$ = 0.6 + 0.347 tan θ
bkgd	0.25 ($\Delta\theta$) at each end	0.25 ($\Delta\theta$) at each end
horizontal aperture, mm	4.0 + 1.0 tan θ (variable)	2.0 + 1.0 tan θ (variable)
reflcns collected	3202	3243
unique reflcns	2851	2904

[a] Unit cell parameters and their esd's were determined from high-angle reflections (24° < 2θ < 26°). [b] Unit cell parameters and their esd's were determined from high-angle reflections (27° < 2θ < 30°).

Table III. Positional Parameters and Their Estimated Standard Deviations for 1[a]

atom	x	y	z	B, Å^2
Ta	0.29179 (4)	0.03908 (7)	0.20762 (3)	3.773 (9)
Cl1	0.3191 (3)	−0.2180 (5)	0.2594 (3)	6.58 (9)
Cl2	0.2039 (3)	0.2488 (5)	0.2488 (3)	7.3 (1)
Cl3	0.3844 (3)	0.1095 (7)	0.3395 (3)	8.5 (1)
Si	0.1313 (3)	−0.0913 (6)	0.2015 (3)	5.4 (1)
C1	0.4090 (7)	0.039 (2)	0.1016 (8)	3.9 (2)
C2	0.3710 (9)	0.190 (1)	0.0964 (7)	4.2 (3)
C3	0.2829 (9)	0.174 (2)	0.0550 (7)	4.5 (3)
C4	0.2681 (8)	0.013 (1)	0.0349 (7)	3.9 (3)
C5	0.3482 (9)	−0.069 (1)	0.0643 (8)	4.1 (3)
C6	0.5016 (8)	0.001 (2)	0.138 (1)	6.0 (4)
C7	0.415 (1)	0.343 (2)	0.123 (1)	7.1 (4)
C8	0.223 (1)	0.305 (2)	0.027 (1)	7.2 (4)
C9	0.1969 (9)	−0.052 (2)	−0.0293 (9)	6.8 (4)
C10	0.367 (1)	−0.243 (2)	0.045 (1)	6.4 (4)
C11	0.120 (1)	−0.301 (2)	0.159 (1)	8.7 (5)
C12	0.0371 (9)	0.021 (3)	0.143 (1)	9.6 (6)
C13	0.110 (1)	−0.091 (2)	0.334 (1)	6.5 (4)
CP1	0.3358	0.0695	0.0704	

[a] Anisotropically refined atoms are given in the form of the isotropic equivalent thermal parameter defined as $(^4/_3)[a^2B(1,1) + b^2B(2,2) + c^2B(3,3) + ab(\cos\gamma)B(1,2) + ac(\cos\beta)B(1,3) + bc(\cos\alpha)B(2,3)]$.

of the Si and P atoms was assigned on the basis of X–C distances observed in related SiMe$_3$[4e,5a,17] and PMe$_3$[18] compounds.

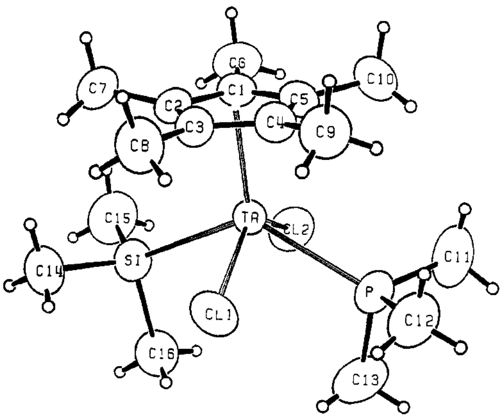

Figure 2. ORTEP view of Cp*Ta(SiMe$_3$)(PMe$_3$)Cl$_2$ (8) showing atom-labeling scheme.

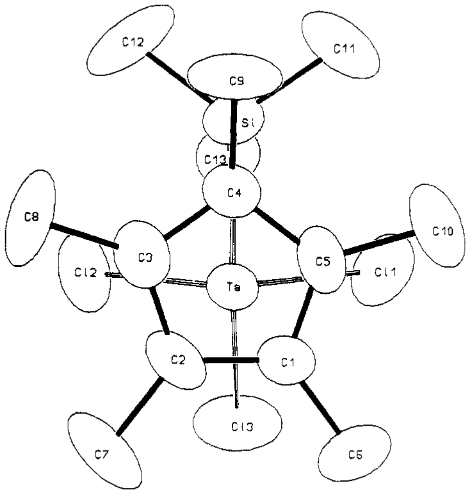

Figure 3. ORTEP view of 1 along the C$_5$Me$_5$ centroid–Ta vector.

Table IV. Positional Parameters and Their Estimated Standard Deviations for 8[a]

atom	x	y	z	B, Å^2
Ta	0.25438 (1)	0.06894 (1)	0.15254 (1)	2.856 (3)
Cl1	0.07930 (7)	0.0120 (1)	0.14317 (7)	5.14 (2)
Cl2	0.34791 (7)	0.2075 (1)	0.24978 (6)	5.01 (2)
P	0.16578 (8)	0.2957 (1)	0.12752 (7)	4.52 (2)
Si	0.2553 (1)	−0.0785 (1)	0.28632 (7)	4.64 (3)
C1	0.4150 (3)	0.0023 (4)	0.1072 (2)	3.70 (8)
C2	0.3576 (3)	−0.1122 (4)	0.1088 (2)	3.58 (8)
C3	0.2736 (3)	−0.0975 (4)	0.0515 (2)	3.77 (8)
C4	0.2788 (3)	0.0257 (4)	0.0131 (2)	3.89 (8)
C5	0.3670 (3)	0.0874 (4)	0.0486 (2)	3.96 (8)
C6	0.5157 (3)	0.0243 (5)	0.1545 (3)	5.7 (1)
C7	0.3922 (3)	−0.2372 (4)	0.1490 (3)	5.2 (1)
C8	0.1965 (3)	−0.1997 (4)	0.0292 (3)	5.7 (1)
C9	0.2105 (4)	0.0719 (5)	−0.0584 (3)	5.8 (1)
C10	0.4101 (3)	0.2131 (5)	0.0204 (3)	6.1 (1)
C11	0.2434 (5)	0.4361 (5)	0.1114 (5)	8.2 (2)
C12	0.0653 (4)	0.3128 (5)	0.0469 (3)	7.0 (1)
C13	0.1039 (4)	0.3378 (5)	0.2210 (3)	7.3 (1)
C14	0.1935 (4)	−0.2423 (5)	0.2781 (3)	6.6 (1)
C15	0.3776 (4)	−0.0984 (5)	0.3519 (3)	7.6 (1)
C16	0.1735 (4)	0.0171 (5)	0.3555 (3)	6.2 (1)
CP1	0.3384	−0.0189	0.0658	

[a] Anisotropically refined atoms are given in the form of the isotropic equivalent thermal parameter defined as $(^4/_3)[a^2B(1,1) + b^2B(2,2) + c^2B(3,3) + ab(\cos\gamma)B(1,2) + ac(\cos\beta)B(1,3) + \mathrm{bc}(\cos\alpha)B(2,3)]$.

As can be seen from Figures 3 and 4 and from angles between least-squares planes (see supplementary material), both molecules possess noncrystallographic C_s symmetry to a high degree. Small differences between the coordination geometries of 1 and 8 are reflected in the angles about the tantalum centers. Relative to 8, 1 has a slight distortion resulting from displacement of C1 and C2 to-

---

(17) (a) Couldwell, M. C.; Simpson, J. *J. Chem. Soc., Dalton Trans.* **1976**, 714. (b) Vancea, L.; Bennett, M. J.; Jones, C. E.; Smith, R. A.; Graham, W. A. G. Inorg. *Chem.* **1977**, *16*, 897.

(18) (a) Luetkens, M. L., Jr.; Elcesser, W. L.; Huffman, J. C.; Sattelberger, A. P. *Inorg. Chem.* **1984**, *23*, 1718. (b) Sattelberger, A. P.; Wilson, R. B., Jr.; Huffman, J. C. *Inorg. Chem.* **1982**, *21*, 4179. (c) Churchill, M. R.; Youngs, W. J. *Inorg. Chem.* **1979**, *18*, 1930.

Table V. Selected Bond Distances (Å) and Angles (deg) for 1[a]

atom 1	atom 2	dist	atom 1	atom 2	dist
Ta	Cl1	2.343 (4)	Si	C13	1.912 (4)
Ta	Cl2	2.314 (4)	C1	C2	1.42 (2)
Ta	Cl3	2.374 (4)	C1	C5	1.39 (2)
Ta	Si	2.669 (4)	C1	C6	1.51 (2)
Ta	C1	2.362 (11)	C2	C3	1.44 (2)
Ta	C2	2.388 (12)	C2	C7	1.50 (2)
Ta	C3	2.449 (11)	C3	C4	1.42 (2)
Ta	C4	2.469 (10)	C3	C8	1.48 (2)
Ta	C5	2.410 (11)	C4	C5	1.45 (2)
Ta	CP1	2.090	C4	C9	1.49 (2)
Si	C11	1.89 (2)	C5	C10	1.54 (2)
Si	C12	1.89 (2)			

atom 1	atom 2	atom 3	angle
CP1	Ta	Cl1	110.4
CP1	Ta	Cl2	110.0
CP1	Ta	Cl3	120.1
CP1	Ta	Si	109.8
Cl1	Ta	Cl2	137.8 (1)
Cl1	Ta	Cl3	84.1 (2)
Cl1	Ta	Si	76.8 (1)
Cl2	Ta	Cl3	86.3 (2)
Cl2	Ta	Si	78.5 (2)
Cl3	Ta	Si	130.0 (1)
Ta	Si	C11	118.3 (6)
Ta	Si	C12	118.5 (7)
Ta	Si	C13	98.9 (5)
C11	Si	C12	106.4 (9)
C11	Si	C13	107.4 (8)
C12	Si	C13	106.0 (7)
C2	C1	C5	109 (1)
C2	C1	C6	126 (1)
C5	C1	C6	126 (1)
C1	C2	C3	108 (1)
C1	C2	C7	127 (1)
C3	C2	C7	125 (1)
C2	C3	C4	108 (1)
C2	C3	C8	126 (1)
C4	C3	C8	126 (1)
C3	C4	C5	107 (1)
C3	C4	C9	126 (1)
C5	C4	C9	125 (1)
C1	C5	C4	109 (1)
C1	C5	C10	125 (1)
C4	C5	C10	125 (1)

[a] CP1 is the centroid of the C_5Me_5 ring.

Table VI. Selected Bond Distances (Å) and Angles (deg) for 8[a]

atom 1	atom 2	dist	atom 1	atom 2	dist
Ta	Cl1	2.402 (1)	Si	C14	1.890 (4)
Ta	Cl2	2.408 (1)	Si	C15	1.890 (5)
Ta	P	2.651 (1)	Si	C16	1.893 (4)
Ta	Si	2.642 (1)	C1	C2	1.415 (5)
Ta	C1	2.412 (3)	C2	C3	1.407 (5)
Ta	C2	2.462 (3)	C3	C4	1.425 (5)
Ta	C3	2.399 (3)	C4	C5	1.423 (5)
Ta	C4	2.334 (3)	C5	C1	1.411 (5)
Ta	C5	2.334 (3)	C1	C6	1.514 (5)
Ta	CP1	2.063	C2	C7	1.508 (5)
P	C11	1.816 (5)	C3	C8	1.502 (5)
P	C12	1.807 (4)	C4	C9	1.495 (5)
P	C13	1.819 (4)	C5	C10	1.509 (5)

atom 1	atom 2	atom 3	angle
CP1	Ta	Cl1	114.89
CP1	Ta	Cl2	115.01
CP1	Ta	P	123.14
CP1	Ta	Si	108.94
Cl1	Ta	Cl2	130.07 (3)
Si	Ta	P	127.91 (3)
Si	Ta	Cl1	81.79 (4)
Si	Ta	Cl2	80.98 (3)
P	Ta	Cl1	77.77 (3)
P	Ta	Cl2	76.90 (3)
Ta	P	C11	118.79 (17)
Ta	P	C12	119.72 (16)
Ta	P	C13	108.09 (15)
C11	P	C12	102.7 (3)
C11	P	C13	102.8 (3)
C12	P	C13	102.4 (2)
Ta	Si	C14	119.15 (14)
Ta	Si	C15	118.25 (16)
Ta	Si	C16	101.91 (14)
C14	Si	C15	107.2 (2)
C14	Si	C16	104.2 (2)
C15	Si	C16	103.8 (2)
C2	C1	C5	108.5 (3)
C2	C1	C6	125.4 (3)
C5	C1	C6	125.9 (3)
C1	C2	C3	107.7 (3)
C1	C2	C7	125.5 (3)
C3	C2	C7	125.4 (3)
C2	C3	C4	108.7 (3)
C2	C3	C8	125.4 (3)
C4	C3	C8	125.7 (3)
C3	C4	C5	107.1 (3)
C3	C4	C9	125.2 (3)
C5	C4	C9	127.3 (3)
C1	C5	C4	108.0 (3)
C1	C5	C10	125.3 (3)
C4	C5	C10	126.1 (3)

[a] CP1 is the centroid of the C_5Me_5 ring.

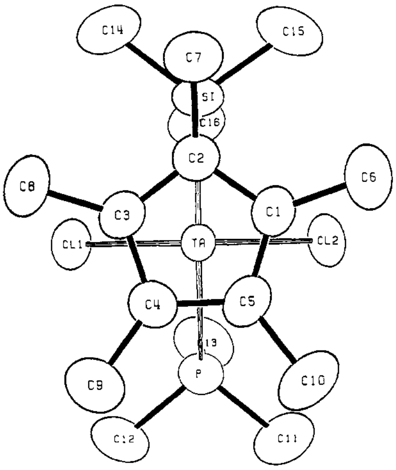

Figure 4. ORTEP view of 8 along the C_5Me_5 centroid–Ta vector.

ward Si and away from each other. These differences most likely result from steric effects. For 8, interactions between the methyl groups on the C_5Me_5 rings and the $SiMe_3$ and PMe_3 ligands appear to be significant, since the C7–C14, C7–C15, C9–C12, and C10–C11 distances (3.481 (6), 3.588 (6), 3.652 (6), and 3.592 (7) Å, respectively) are all shorter than the conventional methyl–methyl nonbonded distance of 4.0 Å.[19] In 1 the C9–C11 and C9–C12 distances are 3.62 (2) and 3.85 (2) Å, respectively. These steric factors may also be responsible for the observed pivoting of the $SiMe_3$ and PMe_3 groups away from the C_5Me_5 ring, resulting in inequivalent Ta–X–C angles.

Structural data for late or low-valent transition-metal silyl derivatives show that metal–silicon distances are shorter than expected for a single covalent bond,[2a,b,d,17] although estimations of covalent single-bond distances are often inaccurate.[2a] This has been attributed to π-bonding involving donation of d-electron density from the transition-metal to silicon. The d^0 silyl complexes $Cp_2Zr(SiPh_3)Cl$[4a] and $Cp_2Zr(SiMe_3)S_2CNEt_2$,[5a] for which such π-bonding is not possible, actually have Zr–Si bond lengths somewhat longer than expected based on covalent radii.

---

(19) Pauling, L. *The Nature of the Chemical Bond*, 3rd ed.; Cornell University Press: Ithaca, NY, 1960.

The latter trend is apparently not general for d^0 silyls, since $Cp_2Ta(SiMe_2Ph)H_2$ contains a "normal" Ta–Si single bond distance.[7] The isolation of tantalum(IV) and tantalum(V) silyl complexes with very similar coordination geometries presented the opportunity to examine the effect of d^n configuration on the metal–silicon bond length.

The Ta–Si bond length in d^0 complex **1**, 2.669 (4) Å, is similar to that found in the more coordinatively saturated $Cp_2Ta(SiMe_2Ph)H_2$, 2.651 (4) Å.[7] The d^1 complex **8** exhibits a shorter Ta–Si bond, 2.642 (1) Å, despite the fact that the covalent radius of the tantalum(IV) center should be greater than that of the tantalum(V) center in **1**. This reduction in bond length of ca. 0.03 Å per d electron may reflect some degree of π-bonding between the Si and Ta in **8**. A similar effect has been observed for metal–phosphine bonding.[20] The Ta–Cl bond lengths show the expected trend, with the average Ta–Cl distance increasing from 2.34 Å in **1** to 2.40 Å in **8**. The Ta–Si single bond distances can be estimated by using the Ta–Cl separations. Given a covalent bond radius of 0.99 Å for Cl,[19] the Ta covalent radii can be calculated as 1.35 Å in **1** and 1.41 Å in **8**. The Si–C distances in these molecules can be combined with the carbon radius of 0.77 Å[19] to calculate a covalent radius of 1.12 Å for Si. The predicted single covalent bond distances are then 2.47 and 2.53 Å for **1** and **8**, respectively. Though the differences in steric and electronic effects in **1** and **8** introduce some error, it appears that both Ta–Si bonds are somewhat elongated, by 0.20 Å in **1** and 0.11 Å in **8**.

Experimental Section

All manipulations were performed under an inert atmosphere of nitrogen or argon. Dry, oxygen-free solvents were employed throughout. Elemental analyses were performed by Galbraith or Schwartzkopf microanalytical laboratories. Infrared spectra were recorded on a Perkin-Elmer 1330 infrared spectrometer. ^1H NMR spectra were recorded at 360 MHz with a spectrometer fabricated locally by Dr. John Wright or at 300 MHz with a GE QE-300. $^{13}C\{^1H\}$ NMR spectra were recorded at 50.3 MHz with a Nicolet WB-200 spectrometer or at 75.5 MHz with a GE QE-300 instrument. GC analyses were conducted on a Varian 3400 instrument coupled to a Varian 4290 integrator, using a 3 m × $^1/_8$ in. stainless-steel column with 25% 1,2,3-tris(2-cyanoethoxy)propane as stationary phase.

$Cp^*Ta(SiMe_3)Cl_3$ (1). A solution of $Al(SiMe_3)_3{\cdot}OEt_2$[8] (12.9 g, 43.7 mmol) in pentane (50 mL) was added to a suspension of Cp^*TaCl_4[9] (20.0 g, 43.7 mmol) in pentane (200 mL). Stirring overnight gave a green solution and a green precipitate. This solution was filtered and the green residue extracted with more pentane until the extracts were colorless. Concentration of the combined pentane extracts and cooling to −45 °C afforded green crystals of the product in 58% yield (12.6 g); mp 130–132 °C. Anal. Calcd for $C_{13}Cl_3H_{24}SiTa$: C, 31.5; H, 4.89; Cl, 21.4. Found: C, 31.6; H, 5.10; Cl, 21.8. IR (Nujol, CsI, cm^{-1}): 1480 s, 1420 m, 1230 s, 1020 s, 828 s, 725 m, 669 s, 605 m, 433 w, 315 s, 273 w.

Reaction of 1 with H_2O. Treatment of a solution of **1** (0.50 g) in diethyl ether (30 mL) with degassed H_2O (0.05 mL) for 12 h resulted in precipitation of a yellow powder. After removal of volatiles, the residue was extracted into dichloromethane (50 mL). The resulting yellow solution deposited a yellow microcrystalline product (0.21 g) upon cooling to −15 °C. Anal. Found: C, 29.3; H, 3.98; Cl, 18.3. ^1H NMR (CD_2Cl_2, 21 °C): δ 2.20 br s. IR (Nujol, CsI, cm^{-1}): 3550 w sh, 2718 w, 1481 m, 1253 w, 1015 s, 828 s, 635 s, 595 s, 468 m, 418 w, 357 s.

$Cp^*Ta(SiMe_3)(OSiMe_3)Cl_2$ (2). Diethyl ether (50 mL) at −78 °C was added to a cold (−78 °C) mixture of **1** (3.0 g, 6.0 mmol) and $KOSiMe_3$ (0.78 g, 6.0 mmol). The resulting red solution was allowed to warm to room temperature and the reaction continued overnight with stirring. Removal of solvent under vacuum followed by extraction with pentane (2 × 30 mL), concentration to ca. 10 mL, and cooling to −15 °C gave the product as red crystals (2.1 g, 64%). Anal. Calcd for $C_{16}Cl_2H_{33}OSi_2Ta$: C, 34.8; H, 6.05; Cl, 12.9. Found: C, 35.0; H, 6.03; Cl, 12.6. IR (Nujol, CsI, cm^{-1}): 1288 m, 1248 s, 1024 w, 915 s, 841 s, 825 s, 755 m, 722 w, 665 w, 612 w, 310 m.

$Cp^*Ta(SiMe_3)(OCMe_3)Cl_2$ (3). The above procedure was followed by using **1** (0.50 g, 1.0 mmol) and $LiOCMe_3$ (0.081 g, 1.0 mmol). The product was obtained as a red microcrystalline powder (0.21 g, 39%). The compound is thermally unstable as a solid and in solution.

$Cp^*Ta(SiMe_3)Me_3$ (4). A solution of MeMgBr (0.96 mL of a 3.2 M diethyl ether solution at room temperature) was syringed into a −78° C solution of **1** (0.50 g, 1.0 mmol) in diethyl ether (30 mL). The red solution was allowed to warm to room temperature and the solvent removed in vacuo. The oily solid was extracted into pentane (3 × 20 mL), and the combined extracts were concentrated (to ca. 10 mL) and cooled to −78 °C. Maroon crystals of the product (0.34 g, 78%) were isolated by filtration. Although the compound decomposes in the solid state within 2 days at ambient temperature, it is stable for long periods (>1 month) at −15 °C, and benzene-d_6 solutions are stable indefinitely at room temperature. IR (Nujol, CsI, cm^{-1}): 1480 m, 1225 s, 1020 m, 830 s, 720 m, 655 m, 608 m, 500 m, 458 m.

$Cp^*CpTa(SiMe_3)Cl$ (5). Diethyl ether (30 mL) at −78 °C was added to a cold (−78 °C) mixture of **1** (1.0 g, 2.0 mmol) and NaCp (0.35 g, 4.0 mmol). After being stirred for 10 min, the resulting suspension was allowed to warm to room temperature and stirring was continued for an additional 4 h. The solvent was removed in vacuo and the dark red residue extracted with pentane (50 mL). Concentration and cooling (−78 °C) of the resulting pentane solution gave the product as maroon crystals (0.43 g, 44%), mp 150–152 °C. Anal. Calcd for $C_{18}ClH_{29}SiTa$: C, 44.1; H, 5.97; Cl, 7.24. Found: C, 44.5; H, 5.85; Cl, 7.58. ESR (benzene-d_6, 25 °C): 8-line pattern (^{181}Ta, $I = {}^7/_2$, 99.988%), $g_{av} = 1.988$, $a_{av} = 7.70 \times 10^{-3}$ cm^{-1}. IR (Nujol, CsI, cm^{-1}): 3120 w, 3091 w, 2720 w, 1241 m, 1224 s, 1022 m, 1010 m, 908 w, 823 s, 737 m, 659 m, 648 m, 608 m, 350 w, 276 m.

$Cp^*CpTa(SiMe_3)(PMe_3)$ (6). A cold (−78 °C) solution of **5** (0.50 g, 1.0 mmol), trimethylphosphine (0.15 mL, 1.6 mmol), and tetrahydrofuran (30 mL) was added to a cold (−78 °C) Na/Hg amalgam (0.023 g of Na, 1.0 mmol, 10 g of Hg). Thirty minutes after the solution was allowed to warm to room temperature with stirring, all volatiles were removed by vacuum transfer leaving an orange residue. Extraction with pentane (2 × 20 mL) followed by concentration to 10 mL and cooling (−45 °C) gave deep red crystals (mp 153–156 °C) of the product in 62% yield (0.33 g). Anal. Calcd for $C_{21}H_{38}PSiTa$: C, 47.5; H, 7.23. Found: C, 46.8; H, 6.71. IR (Nujol, CsI, cm^{-1}): 2505 w, 1271 m, 1228 m, 1210 m, 1103 m, 1017 m, 1001 w, 983 m, 946 s, 829 s, 800 s, 725 m, 708 m, 684 w, 655 m, 627 s, 600 s, 310 m, br.

Reaction of 1 with Alkynes. (a) Diphenylacetylene. A solution of **1** (0.30 g, 0.61 mmol) and $PhC{\equiv}CPh$ (0.11 g, 0.62 mmol) in benzene was refluxed for 2 days. The volatiles were removed by vacuum transfer, leaving an orange residue which dissolved completely in toluene (10 mL). Concentration and cooling (−15 °C) of this solution gave orange crystals of $Cp^*Cl_2Ta(PhC{\equiv}CPh)$[13] in 59% yield. The NMR spectra (CD_2Cl_2, ^1H and $^{13}C\{^1H\}$) were identical with those reported earlier. Analysis of the volatiles from the reaction by GC and ^1H NMR identified Me_3SiCl as an additional product.

(b) Phenylacetylene and 2-Butyne. These reactions were performed in benzene-d_6 or toluene-d_8 at 90 °C in sealed NMR tubes. $Cp^*Cl_2Ta(PhC{\equiv}CH)$: ^1H NMR (benzene-d_6) δ 1.94 (s, 15 H, C_5Me_5), 3.72 (s, 1 H, $PhC{\equiv}CH$), 6.8–7.5 (m, 5 H, $PhC{\equiv}CH$). $Cp^*Cl_2Ta(MeC{\equiv}CMe)$: ^1H NMR (benzene-d_6) δ 1.78 (s, 15 H, C_5Me_5), 2.58 (s, 6 H, $MeC{\equiv}CMe$).

$Cp^*Cl_2Ta(Me_3SiC{\equiv}CSiMe_3)$ (7). After a benzene solution of **1** (0.30 g, 0.61 mmol) and $Me_3SiC{\equiv}CSiMe_3$ (0.7 mL, 3 mmol) was refluxed for 4 h, volatiles were removed in vacuo leaving a purple solid. A tetrahydrofuran extract (10 mL) was concentrated (to ca. 2 mL) and cooled (−45 °C) to yield purple blade-like crystals (30%; mp 165–166 °C). Anal. Calcd for $C_{18}Cl_2H_{33}Si_2Ta$: C, 38.8; H, 5.97; Cl, 12.7. Found: C, 39.0; H, 5.89; Cl, 12.2. IR (Nujol, CsI, cm^{-1}): 1560 m, 1246 m, 915 m, 860 m, 840 s, 750 m, 725 w, 670 m, 383 m, 330 m.

---

[20] Orpen, A. G.; Connelly, N. G. *J. Chem. Soc., Chem. Commun.* **1985**, 1310.

$Cp^*Ta(SiMe_3)(PMe_3)Cl_2$ (8). A solution of **1** (1.00 g, 2.02 mmol) and PMe_3 (0.27 mL, 3.0 mmol) in benzene (10 mL) was stirred at room temperature for 12 h. After removal of the volatiles in vacuo, the brown residue was extracted with pentane (30 mL). The extract solution was concentrated to ca. 15 mL and cooled to −45 °C. The product was isolated as red-brown crystals (mp 127–130 °C) in 55% yield (2 crops, 0.60 g). Anal. Calcd for $C_{16}Cl_2H_{33}PSiTa$: C, 35.8; H, 6.20; Cl, 13.2. Found: C, 35.8; H, 6.35; Cl, 13.1. ESR (benzene-d_6, 20 °C): 8-line pattern (^{181}Ta, $I = {}^7/_2$, 99.988%), $g_{av} = 1.961$, $a_{av} = 9.99 \times 10^{-3}$ cm^{-1}. IR (Nujol, CsI, cm^{-1}): 1412 m, 1275 m, 1020 m, 958 s, 828 s, 730 m, 660 m, 651 m, 600 m, 355 w, 295 s.

Acetonitrile (20 mL) was added to the residue that remained after pentane extraction. Filtration, concentration, and cooling (−45 °C) of this solution gave yellow crystals of $Cp^*TaCl_4(PMe_3)$[12] (2 crops, 0.15 g, 14%).

Reaction of 1 with $Cp^*TaCl_3(PMe_3)$. A solution of **1** (0.50 g, 1.0 mmol) and $Cp^*TaCl_3(PMe_3)$[12] (0.50 g, 1.0 mmol) in benzene (25 mL) was stirred at room temperature for 2 days. The green solution was evaporated to an oily residue, which was extracted with pentane (40 mL). Concentration and cooling (−45 °C) of the pentane solution gave green crystals together with a yellow powder (total weight 0.35 g). ^{1}H NMR analysis of this mixture showed it to contain **1** (70%) and $Cp^*TaCl_4(PMe_3)$ (30%). A beige powder (0.35 g) remaining after pentane extraction could not be characterized.

Reaction of 1 with $Cp^*TaCl_3(PMe_3)$ and PMe_3. Trimethylphosphine (0.089 mL, 1.0 mmol) was added to a solution of **1** (0.50 g, 1.0 mmol) and $Cp^*TaCl_3(PMe_3)$ (0.50 g, 1.0 mmol) in benzene (25 mL) at room temperature. The green solution turned dark red within ca. 30 s. After the solution was stirred for $2^1/_2$ h, the volatiles were removed and the gummy residue was extracted with pentane (40 mL), leaving 0.13 g (0.24 mmol) of $Cp^*TaCl_4(PMe_3)$ (by ^{1}H NMR). Concentration and cooling (−45 °C) of the pentane extract allowed fractional crystallization of more $Cp^*TaCl_4(PMe_3)$ (0.21 g, 0.39 mmol) and **8** (0.35 g, 0.65 mmol, identified by IR, ESR, and melting point).

Reaction of 1 with $Cp^*TaCl_3(PMe_3)$ and PEt_3. Trimethylphosphine was substituted in the above procedure by triethylphosphine. Extraction with pentane (50 mL) left 0.20 g of a beige powder, shown by IR and ^{1}H NMR to be mainly $Cp^*TaCl_4(PMe_3)$. Concentration and cooling (−45 °C) of the pentane solution gave a crop of yellow-green microcrystalline material (0.21 g) shown by ^{1}H NMR to be mainly $Cp^*TaCl_4(PMe_3)$ contaminated slightly by a paramagnetic impurity. More of this paramagnetic compound was obtained as dark red crystals (0.26 g, 0.45 mmol) upon further concentration and cooling of the mother liquor. The spectral properties (IR, ESR) and melting point of this compound were identical with those of a sample of **9** synthesized by the alternate method below.

$Cp^*Ta(SiMe_3)(PEt_3)Cl_2$ (9). Tetrahydrofuran (30 mL) at −78 °C was added to a chilled (−78 °C) mixture of **1** (0.40 g, 0.81 mmol), PEt_3 (0.52 mL, 4.0 mmol) and Na/Hg amalgam (0.019 g, 0.83 mmol, of Na in 10 g of Hg). Allowing the solution to warm to room temperature brought about a color change from green to dark red. The volatiles were removed by evacuation, and the resulting residue was extracted with pentane (2 × 20 mL). Concentration of the combined pentane extracts to ca. 10 mL and cooling (−45 °C) afforded the product as red crystals (0.27 g, 58%), mp 115–117 °C. Anal. Calcd for $C_{19}Cl_2H_{39}PSiTa$: C, 39.4; H, 6.80; Cl, 12.3. Found: C, 39.3; H, 6.81; Cl, 12.5. ESR (benzene-d_6, 25 °C): 8-line pattern, $g_{av} = 1.962$, $a_{av} = 1.32 \times 10^{-2}$ cm^{-1}. IR (Nujol, CsI, cm^{-1}): 2725 w, 1225 m, 1038 m, 1025 m, 830 s, 751 m, 720 m, 666 m, 653 m, 605 m, 420 w, 358 w, 298 s.

Single-Crystal X-ray Diffraction Studies of 1 and 8. Crystals of both compounds were obtained by slow crystallization from cold pentane. The crystals were mounted in thin-walled glass capillaries in an inert-atmosphere glovebox, and the capillaries were flame-sealed. For both crystals the data collection was performed on an Enraf-Nonius CAD-4 diffractometer.[21] In both cases systematic absences were consistent only with space group $P2_1/c$. Automatic peak search and indexing procedures yielded the monoclinic reduced primitive cell. Inspection of the Niggli values[22] revealed no conventional cells of higher symmetry. Final cell parameters and specific data collection parameters are given in Table II. The raw intensity data were converted to structure factor amplitudes and their esd's by correction for scan speed, background, and Lorentz and polarization effects.[23,24] Inspection of the intensity standards showed a monotonic isotropic decrease of the original intensity to 0.94 (for **1**) and 0.95 (for **8**). The data were corrected for this decay. An empirical correction for absorption, based on the azimuthal scan data, was applied to the intensities. The structures were solved by Patterson methods and refined via standard least-squares and Fourier techniques. The quantity minimized by the least-squares program was $\sum w(|F_o| - |F_c|)^2$, where w is the weight of a given operation. The analytical forms of the scattering factor tables for the neutral atoms were used,[25] and all non-hydrogen scattering factors were corrected for both real and imaginary components of anomalous dispersion.[26]

For **1**, some but not all of the hydrogen atoms were located in the structure factor calculations; hydrogens were not included in refinement. The p factor, used to reduce the weight of intense reflections, was set to 0.05 in the final cycles of refinement. The final residuals[27] for 163 variables refined against the 1959 data for which $I < 3\sigma(I)$ were $R = 3.84\%$, $R_w = 4.38\%$, and GOF = 4.634. Inspection of the residuals ordered in ranges of $(\sin\theta)/\lambda$, $|F_o|$, and parity and value of the individual indexes showed no unusual features or trends. The largest peak in the final difference Fourier map had an electron density of 0.72 e/Å^3.

For **8** a difference Fourier map calculated following refinement of all non-hydrogen atoms with anisotropic thermal parameters showed peaks corresponding to the expected positions of most of the hydrogen atoms. Hydrogens were included in the structure factor calculations in their expected positions on the basis of idealized bonding geometry but were not refined in least squares. All hydrogens were assigned isotropic thermal parameters 1–2 Å^2 larger than the equivalent B_{iso} of the atom to which they were bonded. Just prior to the last cycles, it was noted that one reflection (the 3,0,0) had an extraordinarily large value of $W\Delta F^2$. It was eliminated from the refinement. The final residuals for 190 variables refined against the 2494 data for which $F^2 > 3\sigma(F^2)$ were $R = 1.54\%$, $R_w = 2.12\%$, and GOF = 1.424. The R value for all 2904 data was 2.38%. Inspection of the residuals ordered in ranges of $(\sin\theta)/\lambda$, $|F_o|$, and parity and value of the individual indexes showed no unusual features or tends. There was no convincing evidence of secondary extinction in the low-angle, high-intensity data. The largest peak in the final difference Fourier map had an electron density of 0.28 e/Å^3 and was located near the Ta atom. The identities of the Si and P atoms were assigned based on X–C distances observed in other, similar structures.

Acknowledgment is made to the donors of the Petroleum Research Fund, administered by the American Chemical Society, to Research Corp., and to the Air Force Office of Scientific Research (Grant No. AFOSR-85-0228) for support of this work. We thank Mr. M. J. Therien and Prof. R. A. Jones for helpful discussions.

Registry No. **1**, 104155-16-0; **2**, 104155-17-1; **3**, 104155-18-2; **4**, 104155-19-3; **5**, 104155-20-6; **6**, 104155-21-7; **7**, 104155-22-8; **8**,

---

(21) The crystal structure of **1** was determined at the University of Texas. The crystal structure of **8** was determined by Dr. F. J. Hollander, staff crystallographer at the U.C. Berkeley Crystallographic Facility (CHEXRAY), which consists of two Enraf-Nonius CAD-4 diffractometers.

(22) Roof, R. B., Jr. *A Theoretical Extension of the Reduced-Cell Concept in Crystallography*, Publication LA-4083; Los Alamos Scientifc Laboratory: Los Alamos, NM, 1969.

(23) Structure Determination Package User's Guide, 1982; B. A. Frenz and Associates: College Station, TX 77840.

(24) The data reduction formulas (see ref 22) are $F_o^2 = (\omega/Lp)(C - 2B)$, $\sigma_o(F_o^2) = (\omega/Lp)(C + 4B)^{1/2}$, $F_o = (F_o^2)^{1/2}$, and $\sigma_o(F) = \sigma_o(F_o^2)/2F_o$.

(25) Cromer, D. T.; Waber, J. T. *International Tables for X-ray Crystallography*; The Kynoch Press: Birmingham, England, 1984; Vol. IV, Table 2.2B.

(26) Cromer, D. T., ref 25, Table 2.3.1.

(27) $R = \sum|F_o| - |F_c|/\sum|F_o|$, $R_w = \{\sum w(|F_o - F_c|)^2/wF_o^2\}^{1/2}$, and GOF $= \{\sum w(|F_o| - |F_c)^2/(n_o - n_v)\}^{1/2}$ (see ref 23).

104155-23-9; **9**, 104155-24-0; $Al(SiMe_3)_3 \cdot OEt_2$, 75441-10-0; Cp^*TaCl_4, 71414-47-6; $Cp^*TaCl_3(PMe3)$, 71414-45-4; $Cp^*Cl_2Ta(PhC{\equiv}CPh)$, 75522-28-0; $Cp^*Cl_2Ta(PhC{\equiv}CH)$, 75522-33-7; $Cp^*Cl_2Ta(MeC{\equiv}CMe)$, 75522-31-5; $Cp^*TaCl_4(PMe_3)$, 71414-46-5; $PhC{\equiv}CPh$, 501-65-5; $PhC{\equiv}CH$, 536-74-3; $MeC{\equiv}CMe$, 503-17-3; $Me_3SiC{\equiv}CSiMe_3$, 14630-40-1.

Supplementary Material Available: Tables of general temperature factor expressions for 1 and 8, positional parameters for the hydrogen atoms of 8, and least-squares planes for 1 and 8 (5 pages); a listing of observed and calculated structure factors for 1 and 8 (26 pages). Ordering information is given on any current masthead page.

A Comparative Study of Isostructural Palladium and Platinum Methyl Complexes. The Structures of *cis*-Dimethylbis(diphenylmethylphosphine)palladium(II) and *cis*-Dimethylbis(diphenylmethylphosphine)platinum(II)

Jean M. Wisner, Tadeusz J. Bartczak, and James A. Ibers*

Department of Chemistry, Northwestern University, Evanston, Illinois 60201

Received February 28, 1986

The structures of *cis*-dimethylbis(diphenylmethylphosphine)palladium(II) and *cis*-dimethylbis(diphenylmethylphosphine)platinum(II) have been determined crystallographically at −162 °C. The palladium complex crystallizes from acetone in the monoclinic space group C_{2h}^5—$P2_1/c$ with four formula units in a unit cell of dimensions a = 8.882 (3) Å, b = 26.500 (7) Å, c = 11.168 (4) Å, and β = 108.27 (4)°. The structure has been refined to an R index on F^2 of 0.038 for 4799 observations and 280 variables. The platinum congener crystallizes from a benzene/ethanol mixture with four molecules in the space group C_{2h}^5—$P2_1/c$ of the monoclinic system in a cell of dimensions a = 8.859 (4) Å, b = 26.302 (10) Å, c = 11.215 (5) Å, and β = 108.60 (2)°. The Pt structure has been refined to an R index on F^2 of 0.078 for 7678 observations and 280 variables. Both complexes possess slightly distorted square-planar geometry: P(1)–Pd–P(2) = 98.24 (4)°, P(1)–Pt–P(2) = 97.75 (6)°, C(1)–Pd–C(2) = 82.9 (1)°, and C(1)–Pt–C(2) = 81.9 (2)°. Some important bond distances are as follows: Pd–C = 2.089 (3), 2.090 (3) Å; Pt–C = 2.122 (6), 2.119 (5) Å; Pd–P = 2.326 (1), 2.321 (1) Å; Pt–P = 2.285 (2), 2.284 (2) Å. Comparison of the two structures shows a lengthening of the M–C bonds and a concomitant shortening of the M–P bonds when the central metal is changed from palladium to platinum. These structural data are correlated with differences in reactivity. In addition, sets of isostructural compounds in other metal triads are surveyed for analogous trends in bond distances.

Introduction

Alkyl complexes of the d^8 transition metals are believed to be intermediates in a variety of important catalytic processes, including the hydrogenation and carbonylation of organic species.[1] Both palladium and platinum metals in the +II oxidation state form a vast array of square-planar alkyl complexes. However, these complexes often display a significant variation in reactivity and stability. Generally, Pd(II) alkyls are less stable thermodynamically and kinetically than their Pt analogues.[2] Reductive elimination reactions, useful models for catalytic processes forming C–C bonds, are believed to occur more readily for palladium dialkyls.[3]

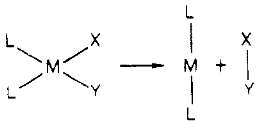

M = Ni, Pd, Pt; X, Y = H, CH_3

We were interested in examining the metal–carbon bonds in an isostructural set of palladium and platinum complexes, in an attempt to correlate structural parameters with reactivity. Here we report an X-ray crystallographic study of *cis*-$Pd(CH_3)_2(P(C_6H_5)_2CH_3)_2$ and *cis*-$Pt(CH_3)_2(P(C_6H_5)_2CH_3)_2$. The choice of these complexes for such a comparative study was dictated by their relative stability and simplicity and by the fact that preliminary crystallographic examination indicated that they are isostructural and have no imposed symmetry. Consequently the effects of crystal packing on the metrical parameters of interest can be assumed to be constant, and the presence of two independent M–Me and M–P bonds in a given structure provides a check on the estimated standard deviations. Such a check is crucial as we anticipated that we would be discussing the significance of small differences between these two structures. Prior to the present study, no structural comparisons of Pd and Pt methyl complexes had been made. In fact, there are only two reports[4,5] of structures with Pd–Me bonds in the literature.

Experimental Section

Dimethylbis(diphenylmethylphosphine)palladium(II) was synthesized by the method of Gillie and Stille[6] and was crystallized from cold acetone. Suitable crystals of the platinum complex were prepared by the published procedure of Bennett, Chee, and Robertson[7] and were crystallized from a 1:1 mixture of dry benzene and absolute ethanol. Both complexes were handled in solution

---

[1] (a) See, for example, James, B. R. *Adv. Organomet. Chem.* **1979**, *17*, 319–405. (b) Heck, R. F. *Acc. Chem. Res.* **1969**, *2*, 10–16.

[2] Komiya, S.; Yamamoto, A.; Yamamoto, T. *Chem. Lett.* **1978**, 1273–1276.

[3] Balazs, A. C.; Johnson, K. H.; Whitesides, G. M. *Inorg. Chem.* **1982**, *21*, 2162–2174. Tatsumi, K.; Hoffmann, R.; Yamamoto, A.; Stille, J. K. *Bull. Chem. Soc. Jpn.* **1981**, *54*, 1857–1867.

[4] Olmstead, M. M.; Farr, J. P.; Balch, A. L. *Inorg. Chim. Acta* **1981**, *52*, 47–54.

[5] Crutchley, R. J.; Powell, J.; Faggiani, R.; Lock, C. J. L. *Inorg. Chim. Acta* **1977**, *24*, L15–L16.

[6] Gillie, A.; Stille, J. K. *J. Am. Chem. Soc.* **1980**, *102*, 4933–4941.

[7] Bennett, M. A.; Chee, H.-K.; Robertson, G. B. *Inorg. Chem.* **1979**, *18*, 1061–1070.

0276-7333/86/2305-2044$01.50/0 © 1986 American Chemical Society